Secure Downlink Transmission to Full-Duplex User Against Randomly Located Eavesdroppers

Ishmam Zabir*, Ahmed Maksud*, Brian M. Sadler† and Yingbo Hua*,
*Department of Electrical and Computer Engineering, University of California, Riverside, CA 92521, USA
†Army Research Laboratory, Adelphi, MD, USA

***Abstract*—We present a statistical analysis of the secrecy capacity for two downlink transmission schemes: transmit-antenna selection (TAS) and transmit-antenna beamforming (TAB), where the transmitter (Alice) has multiple antennas, the receiver (Bob) is a single-antenna full-duplex radio, and the eavesdroppers are randomly distributed each with a single antenna. We focus on the secrecy outage probability (SOP) or its related measure, show closed-form expressions of SOP for the two schemes, and present insights into how various system parameters such as the jamming powers from both Alice and Bob affect SOP. The SOP performance of TAB is shown to be significantly better than that of TAS although TAB requires more on channel estimation than TAS.**

***Index Terms*—Physical layer security, downlink, artificial noise, stochastic geometry, full-duplex, antenna selection, power allocation.**

I. Introduction

Conventional methods for wireless network security are based on cryptography that require a secure channel to distribute secret keys, e.g., see [1]. In the absence of such a secure channel or a pre-existing secret key already shared by (legitimate) users, secure communications between users can be done via physical layer security [2], which has drawn much attention since Wyner's work [3]. One important approach for physical layer security is to ensure that there is a positive secrecy capacity between users against eavesdroppers (Eves).

Achieving positive secrecy is a challenging task when Eves act covertly and their locations are unknown to users. Prior works on physical layer security include cooperative jamming [4], [5], buffer-added relay network [6], exploitation of full-duplex radio [8], [9], [10], and many more [7], [11], [12], [13]. None of those works addresses the situation where Eves' locations are unknown and randomly distributed. One way to handle random locations of Eves is to assume that their locations follow a Poisson point process (PPP) [14]. Such works include [15]-[19], [22].

In this paper, we continue a study in line with [22] where a transmit-antenna selection (TAS) scheme was considered. But unlike [22], we consider a more general situation of TAS where the background noise at the legitimate full-duplex receiver (Bob) is not neglected, which makes it possible to show that there is an optimal value of the jamming power from Bob. Furthermore, we consider a transmit-antenna beamforming (TAB) scheme and show that the secrecy outage probability (SOP) of TAB is significantly better than that of TAS. The expressions of SOP shown in this paper reveal important insights into how various system parameters such as the jamming powers from both Alice and Bob affect the secrecy performance of the system.

Section II presents the system model. Section III studies the performance of the TAS scheme. Section IV investigates the performance of the TAB scheme. Section V presents numerical results.

This work was supported in part by the Army Research Office under Grant Number W911NF-17-1-0581. The views and conclusions contained in this document are those of the authors. Emails: izabi001@ucr.edu, amaks002@ucr.edu, brian.m.sadler6.civ@mail.mil, and yhua@ece.ucr.edu.

II. System Model

We consider a base station (Alice) with M antennas located at the center of a circle of radius R, which transmits secret information to a legitimate receiver (Bob) with a single antenna and full-duplex capability, and located at distance d away from Alice. There are randomly located single-antenna eavesdroppers (Eves) within the circle, and their random locations (denoted by Φ) are modeled as a Poisson point process (PPP) with density ρ_E. The PPP model of Eves is appropriate for long term statistical analysis (such as over hours or days).

The channel gain vector from Alice to Bob is denoted by $\mathbf{h} \in \mathcal{C}^{M\times 1}$, which is normalized such as $\mathbf{h}$ is complex Gaussian with zero mean and identity covariance matrix, i.e., $\mathcal{CN}(\mathbf{0},\mathbf{I})$. A full-duplex radio has self-interference [20], [21], and the self-interference channel gain of Bob is $\sqrt{\rho}g_B$ with the distribution $\mathcal{CN}(0,\rho)$. The channel vector from Alice to the e-th Eve is $\sqrt{a_e}\mathbf{h}_{AE_e} \in \mathcal{C}^{M\times 1}$ and distributed as $\mathcal{CN}(\mathbf{0},a_e\mathbf{I})$, and the channel gain from Bob to e-th Eve is $\sqrt{b_e}h_{BE_e}$ and distributed as $\mathcal{CN}(0,b_e)$.

We also let $a_e = \frac{1}{d^{\alpha}_{AE_e}}$ with d_{AE_e} being the distance between Alice and the e-th Eve, and $b_e = \frac{1}{d^{\alpha}_{BE_e}}$ with d_{BE_e} being the distance between Bob and the e-th Eve. Note that a_e and b_e are large-scale fading parameters as they are dependent on the location of the Eve, while $\mathbf{h}$, g_B, $\mathbf{h}_{AE_e}$ and h_{BE_e} are small-scale fading parameters.

We assume that the single-antenna eavesdroppers cannot collude to form a virtual antenna array while they may share their received information with each other. Then, the secrecy capacity of the downlink transmission from Alice to Bob, conditional on a given set of location of Eves, is

$$S_{AB} = [\log_2(1+SNR_{AB}) - \log_2(1+\max_{e\in\Phi} SNR_{AEe})]^+ \quad (1)$$

where the corresponding signal-to-noise ratios (SNRs) will be discussed later. For a target secrecy rate R_S, the secrecy outage probability (SOP) is defined as

$$P_{out} \doteq P(S_{AB} \leq R_S) = P\left[\frac{1+SNR_{AB}}{1+\max\limits_{e\in\Phi} SNR_{AE_e}} \leq 2^{R_S}\right] \quad (2)$$

where $P(\cdot)$ denotes probability. We will also use $P_{in} \doteq 1 - P_{out}$.

A. Transmit Antenna Selection

In the transmit antenna selection (TAS) scheme, Alice only transmits via the antenna element in $\mathbf{h}$ that has the largest amplitude. Let $\sqrt{P_T}x_A(k)$ of power P_T be the signal transmitted from Alice, and h_{i^*} be the element selected from $\mathbf{h} = [h_1, \cdots, h_M]^T$, i.e., $|h_{i^*}| = \max_i |h_i|$. Thus, Bob and e-th Eve receive the following signals respectively:

$$y_B(k) = h_{i^*}\sqrt{P_T}x_A(k) + \sqrt{\rho P_J}g_B\tilde{w}_B(k) + n_B(k) \quad (3)$$

$$y_{E_e}(k) = \sqrt{a_e P_T}h_{A_{i^*}E_e}x_A(k) + \sqrt{b_e P_J}h_{BE_e}w_B(k) + n_{A_{i^*},E_e}(k) \quad (4)$$

where $\sqrt{P_J}w_B(k)$ of power P_J is the jamming noise from Bob and the jamming signal w_B is Gaussian distributed, $n_B(k)$ and $n_{A_{i^*},E}(k)$ are the background Gaussian noises at Bob and Eve each with the unit variance, and $\sqrt{\rho P_J}g_B\tilde{w}_B(k)$ with instantaneous power $\rho P_J|g_B|^2$ denotes the residual self-interference waveform caused by the original self-interference $\sqrt{P_J}w_B(k)$. Then, the SNR at Bob is

$$SNR_{AB}^{TAS} = \frac{|h_{i^*}|^2 P_T}{1+\rho|g_B|^2 P_J} \quad (5)$$

and the SNR at the e-th Eve is

$$SNR_{AEe}^{TAS} = \frac{a_e|h_{A_{i^*}E_e}|^2 P_T}{1+b_e|h_{BE_e}|^2 P_J} \quad (6)$$

B. Transmit Antenna Beamforming

In the transmit antenna beamforming (TAB) scheme, Alice takes advantage of knowledge of $\mathbf{h}$ by transmitting the following signal:

$$\mathbf{s}(k) = \sqrt{(1-\epsilon)P_T}\mathbf{t}x_A(k) + \sqrt{\frac{\epsilon P_T}{M-1}}\mathbf{W}\mathbf{v}(k) \quad (7)$$

where $x_A(k)$ is the message signal of variance one, $\mathbf{t} = \frac{\mathbf{h}}{\|\mathbf{h}\|}$, $\mathbf{W} \in \mathcal{C}^{M\times(M-1)}$ has orthonormal columns that span the null space of $\mathbf{t}$ (i.e., $\mathbf{t}\mathbf{t}^H + \mathbf{W}\mathbf{W}^H = \mathbf{I}$), $\mathbf{v} \in \mathcal{C}^{(M-1)\times 1}$ is artificial noise $\mathcal{CN}(\mathbf{0}, \mathbf{I})$, and ϵ is the power fraction factor that splits the total power P_T between the message term and the noise term.

Consequently, Bob receives $y_B(k) = \sqrt{(1-\epsilon)P_T}\|\mathbf{h}\|x_A(k) + \sqrt{\rho P_J}g_B\tilde{w}_B(k) + n_B(k)$, and the e-th Eve receives $y_{E_e}(k) = \sqrt{a_e(1-\epsilon)P_T}\frac{\mathbf{h}_{AE_e}^T\mathbf{h}}{\|\mathbf{h}\|}x_A(k) + \sqrt{a_e}\sqrt{\frac{\epsilon P_T}{M-1}}\mathbf{h}_{AEe}^T\mathbf{W}\mathbf{v}(k) + \sqrt{b_e P_J}h_{BE_e}w_B(k) + n_{A,E_e}(k)$. Then, the SNR at Bob is

$$SNR_{AB}^{TAB} = \frac{(1-\epsilon)\|\mathbf{h}\|^2 P_T}{1+\rho|g_B|^2 P_J} \quad (8)$$

and the SNR at the e-th Eve is

$$\begin{aligned} SNR_{AE_e}^{TAB} &= \frac{a_e(1-\epsilon)\frac{|\mathbf{h}_{AE_e}^T\mathbf{h}|^2}{\|\mathbf{h}\|^2}P_T}{1+b_e|h_{BE_e}|^2 P_J + a_e\frac{\epsilon P_T}{M-1}\mathbb{E}_{\mathbf{v}}\{|\mathbf{h}_{AE_e}^T\mathbf{W}\mathbf{v}|^2\}} \\ &= \frac{(1-\epsilon)X_1\Theta P_T}{d_{AE_e}^\alpha + \frac{P_J d_{AE_e}^\alpha}{d_{BE_e}^\alpha}X_2 + \frac{\epsilon P_T}{M-1}X_1(1-\Theta)} \end{aligned} \quad (9)$$

where $\mathbb{E}_{\mathbf{v}}$ denotes the expectation over $\mathbf{v}$, $X_1 = \|\mathbf{h}_{AE_e}\|^2$, $X_2 = |h_{BE_e}|^2$ and $\Theta = \frac{|\mathbf{h}_{AE_e}^T\mathbf{h}|^2}{\|\mathbf{h}_{AE_e}\|^2\|\mathbf{h}\|^2}$. All of the above three random variables are independent of each other. Furthermore, X_1 is Chi-squared distributed with $2M$ degrees of freedom (DoF), i.e., its probability density function (PDF) is $f_{X_1}(x) = \frac{x^{M-1}e^{-x}}{\Gamma(M)}$, X_2 is Chi-squared distributed with 2 DoF (also referred to as exponential distribution of unit mean), and Θ is known to have the Beta$(1, M-1)$ distribution [10], i.e., $f_\Theta(x) = (M-1)(1-x)^{M-2}$.

In order to maintain a data rate R_D from Alice to Bob, we must have $\log_2(1+SNR_{AB}^{TAB}) > R_D$ which implies

$$1-\epsilon > \frac{1+\rho|g_B|^2 P_J}{\|\mathbf{h}\|^2 P_T}(2^{R_D}-1) \quad (10)$$

III. Performance of the TAS Scheme

The performance of the TAS scheme was analyzed in [22] by assuming that the noise at each node is dominated by the interference. In the following, we do not use this assumption. A novelty of the following analysis is that there is generally a nonzero optimal P_J. This insight was not possible to obtain in [22] where the noise was ignored.

We will use the following parameterizations: $\beta = 2^{R_s}$, $m = \frac{P_J}{P_T}$, $Y_0 = \frac{Y}{\beta} + \frac{1}{\beta} - 1$ and

$$Y = \frac{|h_{i^*}|^2}{\frac{1}{P_T} + \rho m|g_B|^2}. \quad (11)$$

Note that for any given $\mathbf{h}$ and g_B, Y is given. Hence, $P[S_{AB}^{TAS} > R_s|\Phi, \mathbf{h}, g_B] = P[S_{AB}^{TAS} > R_s|\Phi, Y]$. Also note that we are only interested in such R_s that $\log_2(1+SNR_{AB}) \geq R_s$ which is equivalent to $Y_0 \geq 0$.

It follows from (1), (5) and (6) that

$$\begin{aligned} P_{in,\Phi,Y} &\doteq P[S_{AB}^{TAS} > R_s|\Phi, Y] \\ &= P\left[\left.\frac{1+SNR_{AB}^{TAS}}{1+\max\limits_{e\in\Phi} SNR_{AE_e}^{TAS}} > 2^{R_S}\right|\Phi, Y\right] \\ &= P\left[\left.\max_{e\in\Phi} SNR_{AE_e}^{TAS} < Y_0\right|\Phi, Y\right] \\ &= \prod_{e\in\Phi} P\left[\left.\frac{|h_{A_{i^*}E_e}|^2}{\frac{d_{AE_e}^\alpha}{P_T} + \frac{d_{AE_e}^\alpha}{d_{BE_e}^\alpha}m|h_{BE_e}|^2} < Y_0\right|\Phi, Y\right] \\ &= \prod_{e\in\Phi}\left(1 - \Psi(Y, r_e, \theta_e)\right) \end{aligned} \quad (12)$$

where

$$\Psi(Y, r_e, \theta_e) = \frac{\exp(-\frac{d_{AE_e}^\alpha}{P_T}Y_0)}{1+m(\frac{d_{AE_e}}{d_{BE_e}})^\alpha Y_0} \quad (13)$$

and (r_e, θ_e) are the polar coordinates of the location of the e-th Eve with the origin at the location of Alice. We have applied the following fact to obtain $\Psi(Y, r_e, \theta_e)$. If A and B (like $|h_{A_{i^*}E_e}|^2$ and $|h_{BE_e}|^2$) are two independent random variables with the exponential distribution of unit mean, then $P(\frac{A}{a+bB} < c) = 1 - \frac{e^{-ac}}{1+bc}$.

Let $P_{in,Y}$ be P_{in} conditional on Y. Applying Campbell's theorem [25] to (12) yields

$$\begin{aligned} P_{in,Y} &= \mathbb{E}_\Phi\{P[SNR_{AB}^{TAS} > R_s|\Phi, Y]\} \\ &= \exp\left[-\rho_E \int_0^R \int_0^{2\pi} \Psi(Y, r, \theta) r d\theta dr \right] \quad (14) \end{aligned}$$

The double integral shown above is difficult to simplify in general. But for $R_s = 0$ and $\alpha = 2$, a simplification is shown in Appendix A.

In order to obtain the unconditional P_{in}, we need the distribution of Y. We can show that the cumulative distribution function (CDF) of Y is

$$F_Y(y) = \sum_{i=0}^{M} C_i^M (-1)^i \frac{e^{-\frac{iy}{P_T}}}{1 + iy\rho m} \quad (15)$$

where $C_i^M = \frac{M!}{(M-i)!i!}$. Hence the PDF of Y is

$$f_Y(y) = \sum_{i=0}^{M} C_i^M (-1)^{i+1} i e^{-\frac{iy}{P_T}} \frac{(\frac{iy\rho m}{P_T} + \frac{1}{P_T} + \rho m)}{(1 + iy\rho m)^2} \quad (16)$$

Therefore,

$$P_{in} = P[S_{AB}^{TAS} > R_s] = \int_0^\infty P_{in,y} f_Y(y) dy. \quad (17)$$

One can verify the following statements for $P_T > 0$:

- If $R_s = 0$, then $\Psi(Y, r, \theta)$ is invariant to $P_T > 0$.
- If $R_s = 0$ and ρP_J is a constant, then as P_J increases to ∞, $\Psi(Y, r, \theta)$ decreases monotonically to zero and hence $P_{in,Y}$ increases monotonically to one.
- In a region of small P_J, Y and hence Y_0 are approximately invariant to P_J, but $\Psi(Y, r, \theta)$ decreases as P_J increases and hence $P_{in,Y}$ increases as P_J increases.

A. The Case of $P_J = 0$

Now we consider the case of $P_J = 0$ and assume that $P_T \gg \frac{1-\beta}{|h_{i^*}|^2}$. It follows that $\Psi(Y; r, \theta) = \exp(-\frac{d_{AEe}^\alpha}{P_T} Y_0) = \exp\left(-r^\alpha \frac{|h_{i^*}|^2}{\beta}\right)$. Hence

$$\begin{aligned} \frac{\ln P_{in,Y}}{\rho_E} &= -\int_0^R \int_0^{2\pi} \Psi(Y; r, \theta) r d\theta dr \\ &= -2\pi \int_0^R \exp\left(-r^\alpha \frac{|h_{i^*}|^2}{\beta}\right) r dr \\ &= -\frac{2\pi\beta^{\frac{2}{\alpha}}}{\alpha(|h_{i^*}|^2)^{\frac{2}{\alpha}}} \int_{r=0}^{\frac{R^\alpha(|h_{i^*}|^2}{\beta}} \exp(-z) z^{\frac{2}{\alpha}-1} dz \\ &= -\frac{2\pi\beta^{\frac{2}{\alpha}}}{\alpha(|h_{i^*}|^2)^{\frac{2}{\alpha}}} \gamma\left(\frac{2}{\alpha}, \frac{|h_{i^*}|^2 R^\alpha}{\beta}\right) \quad (18) \end{aligned}$$

where $\gamma(x, y) = \int_0^y z^{x-1} e^{-z} dz$ is the lower incomplete gamma function. From (18), it is clear that $P_{in,Y}$ monotonically decreases as R increases. In particular,

$$\lim_{R\to\infty} \frac{\ln P_{in,Y}}{\rho_E} = -\frac{2\pi\beta^{\frac{2}{\alpha}}}{\alpha(|h_{i^*}|^2)^{\frac{2}{\alpha}}} \Gamma\left(\frac{2}{\alpha}\right) \quad (19)$$

which increases as α increases provided that $\frac{\beta}{|h_{i^*}|^2} > 1$. Here, $\Gamma(x) = \int_0^\infty z^{x-1} e^{-z} dz$. The above result serves as a benchmark corresponding to a half-duplex Bob.

B. The case of $P_J = \infty$

We now consider the case of $P_J = \infty$ and also assume $R_s = 0$ and $\alpha = 2$. In this case, $Y_0 = Y = 0$ and $mY = \frac{|h_{i^*}|^2}{\rho |g_B|^2}$. Then, following a similar derivation as that from (28) to (30), one can verify that

$$\frac{\ln P_{in,Y}}{\rho_E} = -\int_0^R \int_0^{2\pi} \Psi(Y, r, \theta) r d\theta dr = -2\pi \int_{r=0}^R \Bigg(1 - \frac{1}{\sqrt{1 + \rho \frac{|g_B|^2}{|h_{i^*}|^2}(1 + \frac{d}{r})^2} \sqrt{1 + \rho \frac{|g_B|^2}{|h_{i^*}|^2}(1 - \frac{d}{r})^2}}\Bigg) r dr$$

where the integrant converges to $\left(1 - \frac{1}{1+\rho\frac{|g_B|^2}{|h_{i^*}|^2}}\right) r$ as r becomes large. Hence $\lim_{R\to\infty} P_{in,Y} = 0$. This result suggests that P_J should not be too large. Combining this with the third statement below (17) implies that there is generally a finite nonzero optimal P_J.

IV. Performance of the TAB Scheme

In addition to $m = \frac{P_J}{P_T}$ and $\beta = 2^{R_s}$, we will use $Z = \frac{\|\mathbf{h}\|^2}{\frac{1}{P_T} + \rho m |g_B|^2}$, $c = \frac{Z}{\beta P_T} - \frac{(1-\frac{1}{\beta})}{(1-\epsilon)P_T}$, $f_e = (\frac{d_{AE_e}}{d_{BE_e}})^\alpha m$ and $g = \frac{1}{cP_T}$, which are inter-related variables dependent on $\mathbf{h}$, P_T, P_J, ρ and g_B. Unlike f_e, the terms Z, c and g are invariant to the locations of Eves but dependent on the small scale fading $\mathbf{h}$ and g_B. For $m = 0$, Z has a Chi-squared distribution of M DoF. If $m > 0$, we can show that the PDF of Z is

$$f_Z(z) = \frac{M\rho m (z\rho m)^{M-1}}{(1 + z\rho m)^{M+1}} e^{\frac{1}{\rho P_J}} \quad (20)$$

In the following analysis, we will neglect the background noise for Eve (but not for Bob) if $P_J > 0$, which is favorable for Eve (but not for Bob). It follows that

$$\begin{aligned} &P_{in,\Phi,\mathbf{h},g_B} \doteq P[S_{AB} > R_S|\Phi, \mathbf{h}, g_B] \\ &= P\left[\max_{e\in\Phi} SNR_{AE_e}^{TAB} < \frac{SNR_{AB}}{\beta} - (1 - \frac{1}{\beta}) \middle| \Phi, \mathbf{h}, g_B\right] \\ &= P\Bigg[\max_{e\in\Phi} \frac{X_1\Theta}{\frac{P_J d_{AE_e}^\alpha}{d_{BE_e}^\alpha} X_2 + \frac{\epsilon P_T}{M-1} X_1(1-\Theta)} \\ &< \frac{\|\mathbf{h}\|^2}{\beta(1 + \rho|g_B|^2 P_J)} - \frac{1 - \frac{1}{\beta}}{(1-\epsilon)P_T} \Bigg| \Phi, \mathbf{h}, g_B\Bigg] \\ &= \prod_{e\in\Phi} P\left[\frac{X_1\Theta}{\frac{P_J d_{AE_e}^\alpha}{d_{BE_e}^\alpha} X_2 + \frac{\epsilon P_T}{M-1} X_1(1-\Theta)} < c \middle| \Phi, \mathbf{h}, g_B\right] \\ &= \prod_{e\in\Phi} P\left[\Theta < \frac{\frac{\epsilon}{M-1} + f_e \frac{X_2}{X_1}}{\frac{\epsilon}{M-1} + g} \middle| \Phi, \mathbf{h}, g_B\right] \quad (21) \end{aligned}$$

where X_1, X_2 and $\mathbf{\Theta}$ are independent variables as defined below (9). Furthermore, $\frac{X_2}{X_1}$ is known to have the F-distribution [24], i.e., $f_{\frac{X_2}{X_1}}(x) = M(1+x)^{-(M+1)}$. It follows from $f_\Theta(x)$

shown earlier that $F_\Theta(x) = 1-(1-x)^{M-1}$. Then, as shown in Appendix B,

$$P\left[\Theta > \frac{\frac{\epsilon}{M-1}+f_e\frac{X_2}{X_1}}{\frac{\epsilon}{M-1}+g}|\Phi, Z\right] = \frac{1}{(1+\frac{f_e}{g})(1+\frac{\epsilon}{(M-1)g})^{M-1}} \tag{22}$$

Therefore,

$$\begin{aligned} P_{in,\mathbf{h},g_B} &\doteq \mathbb{E}_\Phi\{P[S_{AB} > R_S|\Phi, \mathbf{h}, g_B]\} \\ &= \mathbb{E}_\Phi\left[\prod_{e\in\Phi}\left(1-\frac{1}{(1+\frac{f_e}{g})(1+\frac{\epsilon}{(M-1)g})^{M-1}}\right)\right] \\ &= \exp\left[-\rho_E\int_0^R r\int_0^{2\pi}\Omega(\frac{1}{g};r,\theta)d\theta dr\right] \end{aligned} \tag{23}$$

where

$$\Omega(\frac{1}{g};r,\theta) = \frac{1}{(1+\frac{f_e}{g})(1+\frac{\epsilon}{(M-1)g})^{M-1}} \tag{24}$$

Finally, averaging $P_{in,\mathbf{h},g_B}$ over the distributions of $\mathbf{h}$ and g_B yields

$$\begin{aligned} &P_{in} \doteq P[S_{AB} > R_s] \\ &= \int_{z=0}^{\infty}\exp\left[\frac{1}{\rho P_J}-\rho_E\int_0^R r\int_0^{2\pi}\frac{dz}{\left(1+f_e(\frac{z}{\beta}+\frac{\frac{1}{\beta}-1}{1-\epsilon})\right)}\right. \\ &\left.\times\frac{1}{\left(1+\frac{\epsilon}{M-1}(\frac{z}{\beta}+\frac{\frac{1}{\beta}-1}{1-\epsilon})\right)^{M-1}}d\theta dr\right]\frac{M\rho m(z\rho m)^{M-1}}{(1+z\rho m)^{M+1}} \end{aligned} \tag{25}$$

One can verify the following for $P_T > 0$:

- Note that $(1+\frac{\epsilon}{(M-1)g})^{M-1}$ converges to $e^{\epsilon/g}$ as M increases. For large P_T, $\frac{\epsilon}{g} = \frac{\epsilon P_T\|\mathbf{h}\|^2}{\beta(1+\rho P_J|g_B|^2)}$ and $\frac{f_e}{g} = \left(\frac{d_{AEe}}{d_{BEe}}\right)^\alpha\frac{\|\mathbf{h}\|^2}{\beta(\frac{1}{P_J}+\rho|g_B|^2)}$. So for $\epsilon > 0$, $P_{in,\mathbf{h},g_B}$ converges to one as P_T increases to ∞.
- $P_{in,\mathbf{h},g_B}$ increases as ρ decreases. If $\rho = 0$, $P_{in,\mathbf{h},g_B}$ increases to one as P_J increases to ∞.
- If $\epsilon = 0$, $P_{in,\mathbf{h},g_B}$ increases to one as P_J increases to ∞.
- For given $\epsilon > 0$ and $P_T > 0$, there is a finite positive P_J at which $P_{in,\mathbf{h},g_B}$ is maximized.

A. The case of $P_J = 0$ but $\epsilon \geq 0$

Now we will not neglect the background noise at Eve. With $P_J = 0$ and then $Z = P_T\|\mathbf{h}\|^2$, one can prove

$$\begin{aligned} \frac{\ln P_{in,\mathbf{h},g_B}}{\rho_E} &= -\int_{r=0}^{R}\int_0^{2\pi}\Omega(z;r,\theta)d\theta rdr \\ &= \frac{-2\pi\beta^{\frac{2}{\alpha}}}{\alpha(\|\mathbf{h}\|^2)^{\frac{2}{\alpha}}(1+\frac{\epsilon P_T}{M-1}\frac{\|\mathbf{h}\|^2}{\beta})^{M-1}}\gamma(\frac{2}{\alpha},\frac{R^\alpha\|\mathbf{h}\|^2}{\beta}) \end{aligned} \tag{26}$$

which is proven in Appendix C. Here $\gamma(\frac{2}{\alpha},\frac{R^\alpha\|\mathbf{h}\|^2}{\beta})$ is the lower incomplete gamma function which increases monotonically as R increases. If $\epsilon = 0$, (26) becomes independent of P_T. Since $\|\mathbf{h}\|^2 \geq \max_{i\in M}|h_i|^2$, comparing (26) with (18) shows that the TAB scheme always has a larger P_{in} than the TAS scheme for $P_J = 0$ and $\epsilon \geq 0$.

B. The case of $\alpha = 2$ and $P_J \to \infty$

With $\alpha = 2$ and $P_J \to \infty$ (hence $zm = \frac{\|\mathbf{h}\|^2}{\rho|g_B|^2}$), we have

$$\begin{aligned} &\frac{\ln P_{in,\mathbf{h},g_B}}{\rho_E} = -\int_{r=0}^{R}\int_0^{2\pi}\Omega(z;r,\theta)d\theta rdr = -2\pi\int_{r=0}^{R} \\ &\left(1-\frac{1}{\sqrt{1+\rho\frac{|g_B|^2}{\|\mathbf{h}\|^2}(1+\frac{d}{r})^2}\sqrt{1+\rho\frac{|g_B|^2}{\|\mathbf{h}\|^2}(1-\frac{d}{r})^2}}\right)rdr \end{aligned} \tag{27}$$

Comparing (20) and (27) once again shows that the TAB scheme has a larger P_{in} than the TAS scheme.

V. Simulations

Here, we assume that $\alpha = 2$ (path loss exponent), $P_T =$ 40dB (transmission power from Alice), $R_D = 4$ (data rate from Alice to Bob in bits/s/Hz), $\rho_E = 1$ (Eve's spatial density), $d = 1$ (distance from Alice to Bob), $R = 5$ (radius of interest) and $M = 5$ (number of antennas on Alice). Unless otherwise specified, P_J (jamming power from Bob), ρ (self-interference gain) and ϵ (fraction of power for jamming noise from Alice) are set to 40dB, 0.01 and 0.01, respectively. Note that ϵ must meet the condition of (10).

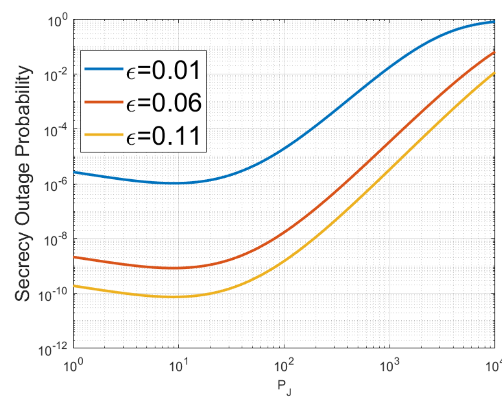

Fig. 1. Illustration of $P_{out} = 1-P_{in}$ versus P_J and ϵ for the TAB scheme.

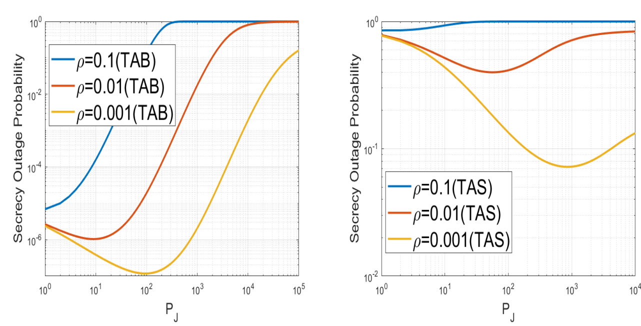

Fig. 2. Comparison between the TAB and TAS schemes in terms of P_{out} .

Fig. 1 illustrates the outage probability P_{out} versus P_J and for different values of ϵ for the TAB scheme. We see that P_{out} decreases as ϵ increases (subject to (10)), and there is an optimal value of P_J for each ϵ. Note that the optimal value of P_J is not sensitive to ϵ.

Fig. 2 compares the TAB and TAS schemes in terms of P_{out}. We see that the performance of TAB is substantially better than that of TAS. In both schemes, P_{out} decreases as ρ decreases, and the optimal value of P_J increases as ρ decreases. We also see that under the same condition, the optimal value of P_J for TAS is larger than that for TAB.

VI. Conclusion

We have studied the secrecy performance of transmit-antenna selection (TAS) and transmit-antenna beamforming (TAB) schemes. In both schemes, the transmitter (Alice) has multiple antennas, the receiver (Bob) is a single-antenna full-duplex radio capable of receiving information and transmitting jamming noise at the same time, and there are randomly located single-antenna eavesdroppers (Eve). We derived closed-form expressions of the secrecy outage probability (SOP) or its related measure for the two schemes subject to Rayleigh fading channels and a PPP distribution of Eve's locations. A number of important insights have been revealed in this paper, including that TAB is much more superior than TAS in terms of SOP, and there is generally an optimal value of the jamming power from Bob.

Appendix A
A simplification of the double integral in (14)

Assume $R_s = 0$ and $\alpha = 2$. Then, $\beta = 1$ and $Y_0 = Y$. Let the distance between Alice and Bob be d. Then, $\frac{d_{AE}^{\alpha}}{d_{BE}^{\alpha}} = \frac{r^2}{r^2+d^2-2rd\cos\theta}$, and furthermore

$$\begin{aligned}
&\int_0^R dr \int_0^{2\pi} d\theta \Psi(Y,r,\theta) r \\
= &\int_0^R dr \int_0^{2\pi} d\theta \frac{\exp(-\frac{Yr^2}{P_T})}{1+mY\frac{r^2}{r^2+d^2-2rd\cos\theta}} r \\
= &\int_0^R dr \int_0^{2\pi} d\theta \exp(-\frac{Yr^2}{P_T}) r \\
&\cdot \frac{(1+mY)r^2+d^2-2rd\cos\theta - mYr^2}{(1+mY)r^2+d^2-2rd\cos\theta} \\
= & 2\pi \int_0^R \exp(-\frac{Yr^2}{P_T}) r dr - \\
&\int_0^R dr \int_0^{2\pi} d\theta \frac{mYr^3\exp(-\frac{Yr^2}{P_T})}{(1+mY)r^2+d^2-2rd\cos\theta}
\end{aligned} \quad (28)$$

where the first term can be obviously reduced, but to simplify the second term we need the following identity

$$\int_0^{2\pi} \frac{1}{a-b\cos\theta} d\theta = \frac{2\pi}{\sqrt{a^2-b^2}} \quad (29)$$

which is proved as follows. Using $\cos(2x) = \frac{1-\tan^2 x}{1+\tan^2 x} = \frac{1-\tan^2 x}{\sec^2 x}$, we can write $\int_0^{2\pi} \frac{1}{a-b\cos\theta} d\theta = 2\int_0^{\pi} \frac{1}{a-b\cos\theta} d\theta = 4\int_0^{\pi/2} \frac{dx}{a-b\cos(2x)} = 4\int_0^{\pi/2} \frac{\sec^2 x}{a+b+(a-b)\tan^2 x} dx = 4\int_0^{\infty} \frac{dy}{a+b+(a-b)y^2} = \frac{4}{\sqrt{a^2-b^2}} \tan^{-1} \frac{y}{\sqrt{\frac{a+b}{a-b}}} \Big|_0^{\infty} = \frac{2\pi}{\sqrt{a^2-b^2}}$.

With (29), (28) becomes

$$\begin{aligned}
&\int_0^R dr \int_0^{2\pi} d\theta \Psi(Y,r,\theta) r \\
= &\frac{\pi P_T}{Y}(1-\exp(-\frac{YR^2}{P_T})) \\
&-2\pi mY \int_0^R \frac{r^3 \exp(-\frac{Yr^2}{P_T}) dr}{\sqrt{\left((1+mY)r^2+d^2\right)^2 - 4r^2d^2}} \\
= &\frac{\pi P_T}{Y}\left(1-\exp(-\frac{YR^2}{P_T})\right) \\
&-\pi mY \int_0^{R^2} \frac{\exp(-\frac{Yr}{P_T}) r dr}{\sqrt{\left((1+mY)r+d^2\right)^2 - 4rd^2}}
\end{aligned} \quad (30)$$

which is a much simplified expression of the double integral in (14).

Appendix B
Proof of (22)

$$\begin{aligned}
&P[\Theta < \frac{\frac{\epsilon}{M-1} + f_e\frac{X_2}{X_1}}{\frac{\epsilon}{M-1}+g} | \Phi, \mathbf{h}, g_B] \\
= &\int_{x=0}^{x=\frac{g}{f_e}} F_{\Theta}(\frac{\frac{\epsilon}{M-1}+f_e x}{\frac{\epsilon}{M-1}+g}) f_{\frac{X_2}{X_1}}(x) dx + 1 - F_{\frac{x_2}{X_1}}(\frac{g}{f_e}) \\
= &\int_{x=0}^{x=\frac{g}{f_e}} \left(1-(1-\frac{\frac{\epsilon}{M-1}+f_e x}{\frac{\epsilon}{M-1}+g})^{M-1}\right) f_{\frac{X_2}{X_1}}(x) dx \\
+ &\ 1 - F_{\frac{x_2}{X_1}}(\frac{g}{f_e}) \\
= &\ 1 - \frac{Mg^{M-1}}{(\frac{\epsilon}{M-1}+g)^{M-1}} \int_{x=0}^{x=\frac{g}{f_e}} \left(\frac{1-\frac{f_e}{g}x}{1+x}\right)^{M-1} \frac{dx}{(1+x)^2}
\end{aligned} \quad (31)$$

With $k = \frac{f_e}{g}$ and $z = \frac{1}{1+x}$, $(\frac{1-kx}{1+x})^{M-1} = k^{M-1}\big(-1 + z\frac{k+1}{k}\big)^{M-1}$ then

$$\begin{aligned}
&P[\Theta < \frac{\frac{\epsilon}{M-1} + f_e\frac{X_2}{X_1}}{\frac{\epsilon}{M-1}+g} | \Phi, \mathbf{h}, g_B] \\
= &\ 1 - \frac{Mg^{M-1}}{(\frac{\epsilon}{M-1}+g)^{M-1}} \int_{x=0}^{x=\frac{g}{f_e}} (\frac{1-\frac{f_e}{g}x}{1+x})^{M-1} \frac{dx}{(1+x)^2} \\
= &\ 1 - \frac{M(gk)^{M-1}}{(\frac{\epsilon}{M-1}+g)^{M-1}} \int_{z=\frac{k}{k+1}}^{z=1} \big(z(\frac{k+1}{k}-1)\big)^{M-1} dz \\
= &\ 1 - \frac{Mk^M}{(1+k)(1+\frac{\epsilon}{(M-1)g})^{M-1}} \int_{y=0}^{y=\frac{1}{k}} y^{M-1} dy \\
= &\ 1 - \frac{1}{(1+\frac{f_e}{g})(1+\frac{\epsilon}{(M-1)g})^{M-1}}
\end{aligned} \quad (32)$$

Appendix C
Proof of (26)

With $P_J = 0$, $c \approx \frac{\|\mathbf{h}\|^2}{\beta}$ for high P_T and $z = P_T\|\mathbf{h}\|^2$, and

$$\begin{aligned} & P[S_{AB} > R_S|\Phi, \mathbf{h}, g_B] \\ = & \prod_{e\in\Phi} P\big[\frac{X_1\Theta}{d^{\alpha}_{AE_e} + \frac{\epsilon P_T}{M-1}X_1(1-\Theta)} < c|\Phi, \mathbf{h}, g_B\big] \\ = & \prod_{e\in\Phi} P\big[\frac{X_4}{d^{\alpha}_{AE_e} + \frac{\epsilon P_T}{M-1}X_3} < \frac{\|\mathbf{h}\|^2}{\beta}|\Phi, \mathbf{h}, g_B\big] \end{aligned} \quad (33)$$

where $X_4 = \Theta X_1 = \frac{|\mathbf{h}_{AE_e} T\mathbf{h}|^2}{\|\mathbf{h}\|^2}$ is exponentially distributed with mean equal to 1, and $X_3 = (1-\Theta)X_1 = \mathbb{E}_{\mathbf{v}}|\mathbf{h}^T_{AE_e}\mathbf{W}\mathbf{v}|^2$ follows the $\Gamma(M-1, 1)$ distribution. Furthermore, X_3 and X_4 are independent. Then,

$$\begin{aligned} & P\big[\frac{X_4}{d^{\alpha}_{AE_e} + \frac{\epsilon P_T}{M-1}X_3} < \frac{\|\mathbf{h}\|^2}{\beta}|\Phi, \mathbf{h}, g_B\big] \\ = & 1 - \int_0^{\infty} F_{X_4}\big(\frac{\|\mathbf{h}\|^2}{\beta}d^{\alpha}_{AE_e} + \frac{\|\mathbf{h}\|^2}{\beta}\frac{\epsilon P_T y}{M-1}\big) f_{X_3}(x)dx \\ = & 1 - \frac{e^{-\frac{\|\mathbf{h}\|^2}{\beta}d^{\alpha}_{AE_e}}}{\Gamma(M-1)} \int_0^{\infty} e^{-(1+\frac{\|\mathbf{h}\|^2}{\beta}\frac{\epsilon P_T}{M-1})y} y^{M-2} dy \\ = & 1 - \frac{e^{-\frac{\|\mathbf{h}\|^2}{\beta}d^{\alpha}_{AE_e}}}{(1+\frac{\|\mathbf{h}\|^2}{\beta}\frac{\epsilon P_T}{M-1})^{M-1}} \\ = & 1 - \frac{e^{-\frac{z}{\beta}\frac{d^{\alpha}_{AE_e}}{P_T}}}{(1+\frac{z}{\beta}\frac{\epsilon}{M-1})^{M-1}} \end{aligned} \quad (34)$$

Now,

$$\begin{aligned} & \int_{r=0}^{R}\int_0^{2\pi} \Omega(z; r, \theta) d\theta r dr \\ = & \frac{2\pi}{(1+\frac{z}{\beta}\frac{\epsilon}{M-1})^{M-1}} \int_{r=0}^{R} e^{-\frac{z}{\beta}\frac{r^{\alpha}}{P_T}} r dr \\ = & \frac{2\pi\beta^{\frac{2}{\alpha}}}{\alpha(\|\mathbf{h}\|^2)^{\frac{2}{\alpha}}(1+\frac{\epsilon P_T}{M-1}\frac{\|\mathbf{h}\|^2}{\beta})^{M-1}} \int_{y=0}^{\frac{R^{\alpha}\|\mathbf{h}\|^2}{\beta}} e^{-y} y^{\frac{2}{\alpha}-1} y dy \\ = & \frac{2\pi\beta^{\frac{2}{\alpha}}}{\alpha(\|\mathbf{h}\|^2)^{\frac{2}{\alpha}}(1+\frac{\epsilon P_T}{M-1}\frac{\|\mathbf{h}\|^2}{\beta})^{M-1}} \gamma\big(\frac{2}{\alpha}, \frac{R^{\alpha}\|\mathbf{h}\|^2}{\beta}\big) \end{aligned} \quad (35)$$

References

[1] E. D. Silva, A. L. D. Santos, L. C. P. Albini, and M. Lima, "Identity based key management in mobile ad hoc networks: Techniques and applications," IEEE Trans. Wireless Commun., vol. 15, no. 5, pp. 46-52, Oct. 2008.

[2] N. Yang, L. Wang, G. Geraci, M. Elkashlan, J. Yuan, and M. D. Renzo, "Safeguarding 5G wireless communication networks using physical layer security," IEEE Commun. Mag., vol. 53, no. 4, pp. 20-27, Apr. 2015.

[3] A. D. Wyner, "The wire-tap channel", Bell Syst. Tech. J., vol. 54, pp. 1355-1387, Jan. 1975.

[4] E. Tekin and A. Yener, "The general gaussian multiple access and twoway wire-tap channels: achievable rates and cooperative jamming," IEEE Trans. Inform. Theory, vol. 54, pp. 2735-2751, June 2008.

[5] H. Zhang, H. Xing, J. Cheng, A. Nallanathan, and V. Leung, "Secure resource allocation for ofdma two-way relay wireless sensor networks without and with cooperative jamming," IEEE Trans. Industrial vol. 12, no. 5, pp. 1714-1725, Oct. 2016.

[6] G. Chen, Z. Tian, Y. Gong, Z. Chen, and J. A. Chambers, "Max-ratio relay selection in secure buffer-aided cooperative wireless networks," IEEE Trans. Inform. Forensics and Security, vol. 9, no. 4, pp. 719-729, Apr. 2014.

[7] H. Weingarten, T. Liu, S. Shamai, Y. Steinberg, and P. Viswanath, "The capacity region of the degraded multiple-input multiple-output compound broadcast channel," IEEE Trans. Inf. Theory, vol. 55, pp. 5011-5023, Nov. 2009.

[8] L. Chen, Q. Zhu, W. Meng and Y. Hua, "Fast Power Allocation for Secure Communication with Full-Duplex Radio", IEEE Transactions on Signal Processing, vol. 65, no. 14, pp. 3846-3861, July 2017.

[9] Y. Hua, Q. Zhu, and R. Sohrabi, "Fundamental Properties of Full-Duplex Radio for Secure Wireless Communications," http://arxiv.org/abs/1711.10001.

[10] Y. Hua, "Advanced Properties of Full-Duplex Radio for Securing Wireless Network," IEEE Transactions on Signal Processing, vol. 67, pp. 120-135, Jan. 2019.

[11] G. Chen, Y. Gong, P. Xiao, and J. A. Chambers, "Dual antenna selection in secure cognitive radio networks," IEEE Trans. Veh. Technol., vol. 65, no. 10, pp. 7993-8002, Oct. 2016.

[12] A. Khisti, G. Wornell, A. Wiesel, and Y. Eldar, "On the Gaussian MIMO wiretap channel," in Proc. IEEE Int. Symp. Information Theory, Nice, France, June 2007.

[13] S. Goel and R. Negi, "Guaranteeing secrecy using artificial noise," IEEE Trans. Wireless Commun., vol. 7, no. 6, pp. 2180-2189, June 2008.

[14] M. Haenggi, "The secrecy graph and some of its properties," in Proc. IEEE Int. Symp. Inf. Theory, Toronto, Canada, pp. 539-543, July 2008.

[15] M. Ghogho and A. Swami, "Physical-layer secrecy of MIMO communications in the presence of a poisson random field of eavesdroppers," in Proc. IEEE ICC, Jun. 2011, pp. 1-5.

[16] G. Geraci, S. Singh, J. G. Andrews, J. Yuan, and I. B. Collings, "Secrecy rates in broadcast channels with confidential messages and external eavesdroppers," IEEE Trans. on Wireless Commun., vol. 13, pp. 2931-2943, May 2014.

[17] T. X. Zheng, H. M. Wang, and Q. Yin, "On transmission secrecy outage of a multi-antenna system with randomly located eavesdroppers," IEEE Commun. Lett., vol. 18, pp. 1299-1302, Aug. 2014.

[18] T. X. Zheng, H. M. Wang, J. Yuan, D. Towsley, and M. H. Lee, "Multiantenna transmission with artificial noise against randomly distributed eavesdroppers," IEEE Trans. on Commun., vol. 63, pp. 4347-4362, Nov. 2015.

[19] T. X. Zheng, H. M. Wang, "Optimal Power Allocation for Artificial Noise Under Imperfect CSI Against Spatially Random Eavesdroppers," IEEE Trans. on Vehicular Technology, vol. 65, pp. 8812 - 8817, Oct. 2016.

[20] T. Riihonen, S. Werner, R. Wichman, "Mitigation of loopback self-interference in full-duplex MIMO relays", IEEE Trans. Signal Process. vol. 59, Dec 2011, 5983-5993.

[21] Y. Hua, Y. Ma, A. Gholian, Y. Li, A. Cirik, P. Liang, "Radio Self-Interference Cancellation by Transmit Beamforming, All-Analog Cancellation and Blind Digital Tuning," Signal Processing, vol. 108, pp. 322-340, 2015.

[22] G. Chen, J. P. Coon and M. D. Renzo, "Secrecy Outage Analysis for Downlink Transmissions in the Presence of Randomly Located Eavesdroppers," IEEE Transactions on Information Forensics and Security, vol. 12, no. 5, pp. 1195-1206, May 2017.

[23] T.-X. Zheng, H.-M. Wang, J. Yuan, D. Towsley, M. H. Lee,"Multi-Antenna Transmission with Artificial Noise Against Randomly Distributed Eavesdroppers", IEEE Transactions on Communications, vol. 63, no. 11, Nov. 2015.

[24] https://en.wikipedia.org/wiki/F-distribution

[25] R.L. Streit, The Poisson Point Process. In: Poisson Point Processes. Springer, Boston, MA, 2010.